CHEMISTRY OF MATERIALS

Article

pubs.acs.org/cm

pH-Dependent Synthesis and Stability of Aqueous, Elemental Bismuth Glyconanoparticle Colloids: Potentially Biocompatible X-ray Contrast Agents

Anna L. Brown[‡] and Andrea M. Goforth[‡,*]

[‡]Department of Chemistry, Portland State University, 1719 SW 10th Ave., Portland, Oregon 97201, United States

Supporting Information

ABSTRACT: Taking advantage of a pH-dependent solubility equilibrium, we have developed an aqueous synthesis of chemically and colloidally stable bismuth(0) glyconanoparticles. The synthetic method results in potentially biocompatible elemental bismuth nanoparticles (BiNPs) and involves the reduction of aqueous bismuth(III) cations by sodium borohydride in a pH-controlled solution. Medical-grade dextran (75 000 MW) was found to protect the nanocrystals from oxidation, in addition to promoting colloidal stability and separation of individual nanocrystallites. The rate of particle formation was dependent on synthesis pH, and decreasing the reaction rate by increasing the pH produced a greater number of individual and isolated Bi(0) nanocrystals. Stable, aqueous colloids of the dextran-coated BiNPs decomposed under prolonged light exposure, and the NPs dissolved both in acidic solutions (pH <7) and highly alkaline solutions (pH >12), but were stable in phosphate buffered saline solution (pH 7.4) and in other aqueous solutions between pH 8 and 10. Bismuth-based nanomaterials have previously been demonstrated to be long-circulating X-ray contrast agents, and we anticipate that these high-atomic-number bismuth(0) glyconanoparticles will find use in similar applications.

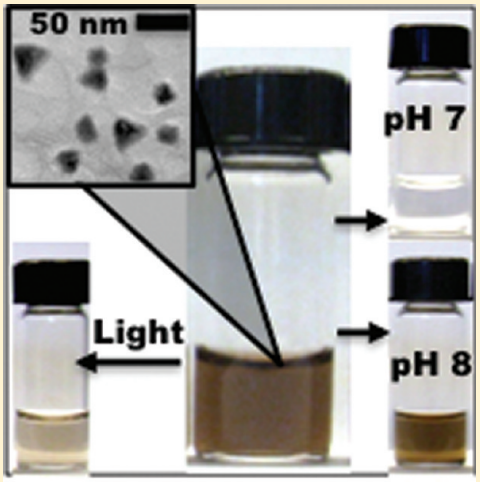

KEYWORDS: *(semi)metal nanoparticles, bismuth nanoparticles, glyconanoparticles, X-ray contrast agents, pH dependence, chemical and colloidal stability, aqueous chemistry of bismuth*

INTRODUCTION

Bismuth nanoparticles (BiNPs) have garnered attention recently, because of their predicted quantum size effects,[1,2] favorable thermoelectric properties,[3−5] and use as seeds for VLS growth of metal nanowires.[6,7] In addition, the potential of Bi-based nanomaterials has very recently been explored as high-contrast, long-circulating, low-toxicity X-ray contrast agents (XCAs).[8−10] Nanometer-sized inorganic particles are attractive as XCAs, because they contain a large number (hundreds or more) of X-ray attenuating atoms in a relatively small volume, which should allow for intravenous administration at low concentrations, particularly if the particles are site-directed by the addition of biological recognition moieties to the surface.[11] The inherent high surface-area:volume ratio characteristic of nanoparticles can be further advantageous in allowing for the addition of high copy numbers of recognition groups to the NP surface, thus taking advantage of recognized multivalency effects in certain nanoparticle-biological structure honing interactions.[12]

Bismuth is an attractive element for nanomaterial XCAs, because of its high atomic number (Z = 83) and well-known biological tolerance.[13] The first of these properties will make bismuth-based contrast agents more X-ray opaque, on a per atom basis, than current, clinically used, iodine-based (Z = 53) contrast agents; the second should allow for safe use during imaging as well as biological clearance after imaging. As an alternative to bismuth-based nanoparticles, heavy-element gold nanoparticles (AuNPs, Z = 79) have begun to be explored as nano XCAs,[14−16] primarily because of the ease of synthesis and morphological control that has been demonstrated for AuNPs over the last several decades. However, gold is currently about 2000 times more expensive per mole[17] and approximately half as terrestrially abundant as bismuth,[18] making AuNPs substantially less attractive than BiNPs for large-scale, systematic medical use.[19] Most importantly, while the oxidative inertness of AuNPs confers a synthetic advantage in the laboratory, AuNPs larger than 5 nm pose a toxicity risk, since they would not be renally cleared,[11] thus making bioaccumulation likely.[20] Conversely, elemental BiNPs readily undergo oxidation and hydrolysis in water, rendering them difficult to synthesize and stabilize in an aqueous environment while simultaneously making them more likely to decompose to small, renally clearable, molecular or ionic Bi(III) species in vivo. Medically, Bi(III)-chelate solutions have been used for

Received: January 9, 2012
Revised: March 30, 2012
Published: April 10, 2012

dx.doi.org/10.1021/cm300083j | *Chem. Mater.* 2012, 24, 1599−1605

centuries in relatively high doses (multiple gram doses per day)[21] as safe antimicrobial and antiemetic treatments with minimal known toxicity, despite the fact that these preparations have been predominantly chemically ill-defined.[13] Bismuth(III) complexes present in blood are thought to be cleared by urinary excretion via metallothionine, which is a cysteine-rich protein abundant in the kidneys that has been shown to have preferential affinity for bismuth over other elements, regardless of pH.[22]

While the hydrolytic instability of BiNPs may prove advantageous for a medical application by providing a mechanism (i.e., biocorrosion) for clearance, aqueous synthesis of BiNPs is a substantial challenge as is the stabilization of aqueous BiNP colloids for a time period suitable as an imaging window (up to 24 h). The majority of BiNP preparations reported to date are carried out anaerobically, using organic solvents and morphology-controlling surfactants of poor or unknown biocompatibility. These syntheses primarily yield hydrophobic BiNPs or present challenges for purification from excess, potentially toxic reagents prior to a biological application. The elegant synthetic preparations of BiNPs by Buhro and others from $Bi(N(SiMe_3)_2)_3$ produce a variety of well-controlled shapes and sizes.[23−25] However, the use of hydrophobic solvents and a specialty block copolymer for stability makes the products of this preparation method nonideal for medical application. Variations of polyol preparations have been reported for the synthesis of Bi nanostructures in ethylene glycol, including spheres,[26,27] cubes,[28] and wires.[29] In these preparations, PVP is used as a surfactant, stabilizer and morphology-directing agent. Although the use of PVP may confer some degree of aqueous stability to the particles after workup, we were unable to find literature evidence that PVP prevents surface oxidation and eventual hydrolysis of elemental BiNPs, which is commensurate with our laboratory experience with this capping agent. A unique, aqueous preparation of BiNPs uses oleate as a surfactant to form a stabilizing barrier against BiNP hydrolysis;[30] however, this hydrophobic barrier also prevents colloidal dispersion of the nanocrystals in water. To date, an aqueous synthesis method employing biocompatible reagents that yields small (<200 nm hydrodynamic radius), colloidally stable, hydrophilic BiNPs has not been reported. An aqueous synthetic preparation (which reduces purification steps and minimizes toxicity risks), hydrophilicity, and intermediate hydrolytic stability are all requisites for a suitable nanomaterial XCA.

Herein, we describe a solution method for the aqueous synthesis and aqueous stabilization of elemental BiNPs, which are produced by a simple, benchtop Bi(III) salt reduction using biocompatible reagents. We also examined the quality (size, morphology, extent of aggregation, and period of colloidal/chemical stability) of the BiNP products to determine synthesis and storage conditions suitable for future utilization of these high-atomic-number NPs in medical imaging. We used $Bi(NO_3)_3{\cdot}5H_2O$ treated with varying amounts of KOH and a standard amount of glycine to control pH and, thus, the concentration of Bi(III) monomer available for reduction. Short-chain medical-grade dextran (75 000 MW) was used as a biocompatible surfactant in the preparation, and sodium borohydride was used as the reducing agent. Dextran is a glucose polymer used medically as a plasma volume enhancer and is also commonly used to solubilize iron as an intravenous treatment for anemia. In this preparation, dextran serves to surface stabilize the BiNPs while promoting colloidal stability in aqueous media and providing reasonably long-term protection against hydrolysis, both of which (colloidal and chemical stability) are observed to be dependent on pH. While the effect of OH^-/Bi(III) ratio on the morphology of Bi nanostructures has been reported in nonaqueous media (i.e., ethylene glycol)[29] and the effect of OH^-/Bi(III) ratio on the kinetics of aqueous bismuth hydroxide ($Bi(OH)_3$) particle formation has been examined,[31] to our knowledge, this work constitutes the first report on the effect of pH in controlling the aqueous synthesis and stability of elemental BiNPs.

EXPERIMENTAL SECTION

Reagents. Bismuth nitrate pentahydrate (Acros, 98%), glycine (Acros, 99+%, analysis grade), KOH (reagent grade), dextran (Carbomer, Inc., 75 000 MW, clinical grade), sodium borohydride (MP Biomedicals, 98%−99%) and phosphoric acid (Sigma−Aldrich, >85%) were purchased and used as received without further purification. All solutions were prepared using fresh, electrophoretically pure H_2O (resistivity = 18 MΩ cm).

Synthesis. All reactions were performed with magnetic stirring at >800 rpm. During the reactions, temperature was held constant at 40 °C by immersion of the reaction vessel (a 100-mL beaker) in a temperature-controlled water bath. In a typical synthesis, 250 mg (0.52 mmol) $Bi(NO_3)_3{\cdot}5H_2O$ was suspended by sonication in 25.0 mL of H_2O. A 2.00 M glycine solution (10.0 mL, 20 mmol) was added to the bismuth(III) solution, along with an appropriate amount of 2.0 M KOH to achieve a specified pH (e.g., 12.0 mL, 12 mmol, for a measured pH of 9.0). Then, 7.5 mL of a 100 mg/mL dextran stock solution (750 mg) was added immediately prior to the addition of 12.5 mL of a freshly prepared 10 mg/mL (3.3 mmol) $NaBH_4$ solution. Upon the addition of reducing agent, the solution was observed to change from a cloudy, colorless suspension to a black solution in a time frame that was dependent on the initial pH of the reaction. After ∼5 min, when the reactions appeared to have stabilized by visual inspection (based on color change) and cessation of gas evolution (H_2 from BH_4^-), all solutions were brought to the same pH (7.4) via the dropwise addition of 1.0 M H_3PO_4. Samples were briefly sonicated to promote dispersion and were stirred for 1 h at room temperature prior to purification.

Dialysis and Purification. The reaction products containing the nanoparticles were dialyzed against water using Spectrum* Spectra/Por (50 000 MWCO) dialysis tubing to separate the nanoparticles from salts, excess starting reagents, and small molecule byproducts. The purified nanoparticle solutions were then centrifuged at 3.0 RCF for 10 min to remove large aggregates. Nanoparticles in the supernatant were concentrated by rotary evaporation under vacuum (40 °C water bath) and stored at room temperature away from light. For long-term storage, samples were stored in water either at −20 °C or at 4 °C with a trace amount of sodium azide to prevent biological contamination.

Spectroscopic Analysis of Particle Nucleation, Growth, and Stability as a Function of pH. In order to monitor the reaction progress as a function of pH spectroscopically, the reaction was scaled down to keep absorbance/scattering values under 2 for the duration of the reactions. A dilute bismuth nitrate stock solution of 2.06 mM dissolved $Bi(NO_3)_3{\cdot}5H_2O$ was prepared and sonicated to optical clarity. Glycine, dextran, and KOH stock solutions were also prepared and were of the same concentrations as used in the larger-scale preparations. Each reaction solution contained a standard final amount of Bi(III) (5.15 μmol), glycine (100 μmol), and dextran (75 mg). KOH was added to achieve desired pH values in the range of 8−10. Preparations for the reactions took place in the following order: (1) appropriate volumes of the Bi(III), glycine, and KOH solutions were added to and mixed in 8.0 mL of H_2O, (2) the pH was measured, (3) dextran solution was added, and (4) H_2O was added as needed to bring the final volume of each solution to 9.9 mL. Each sample was then divided into three, equal-volume aliquots, which were monitored simultaneously by UV−visible spectroscopy on a Varian Cary 100 Bio

equipped with stirring capabilities. Light attenuation (due to absorption *and* scattering by the BiNPs) was measured at 650 nm every 5 s after the addition of sodium borohydride solution (37.5 μL, 10.57 μmol) to each cuvette at time t = 0 s. Data was collected simultaneously from replicates at each pH and recorded in parallel. Attenuation values at each time point from the three replicates for each pH were averaged and plotted versus elapsed time. For consistency, all samples were prepared, mixed, and measurements initiated within 90 s.

Though all reaction conditions were not exactly identical to those used in the large-scale preparations due to measurement requirements, these small-scale spectroscopic experiments allow real-time observation of reaction stages and trends in reaction progress (i.e., rates) as a function of pH; qualitatively, the same trends in nucleation periods and growth rates are observed in the large-scale preparations, although the colloids produced in the large-scale preparations generally are colloidally stable for longer time periods (days versus hours).

Product Characterization. Ultraviolet-visible light (UV−vis) spectra for the products of the large-scale preparations were collected on a Shimadzu Model UV-2450 UV−vis spectrophotometer in standard 1-cm disposable polystyrene cuvettes.

Dynamic light scattering (DLS) measurements were obtained using a Horiba LB-550 DLS instrument. Samples were purified as described above, diluted in water, and passed through a 0.45-μm polytetrafluoroethylene (PTFE) syringe filter prior to measurement. Measurements (300 scans) at five different concentrations of each sample were performed in order to determine a size distribution independent of concentration effects (e.g., multiple scattering).

Transmission electron microscopy (TEM) was performed on an FEI Tecnai F-20 TEM operating at 200 kV. Purified samples were drop-cast on Ted Pella holey carbon copper-supported grids and dried for 2 h at 150 °C prior to imaging. Energy-dispersive X-ray (EDX) spectroscopy was performed on a representative sample on 20 individual particles during TEM imaging.

Fourier transform infrared (FT-IR) spectroscopy was performed on a Thermo Scientific Nicolet iS10 spectrophotometer equipped with a single-bounce diamond ATR attachment. Aqueous solutions of purified Bi NPs, dextran, and glycine were drop-cast onto the ATR crystal and the solvent was evaporated as necessary using a heat gun to deposit a sample film for analysis.

For XRD analysis, concentrated BiNP samples were evaporated to dryness in a ceramic evaporation dish in air, milled into a fine powder, and pressed onto a glass slide. Data were collected in focused beam (Bragg−Brentano) geometry on a Rigaku Model Ultima IV X-ray diffraction system using graphite-monochromatized Cu Kα radiation. Scans were performed over the angular range of 5°−85° 2θ at a scan rate of 0.25°/min at room temperature.

RESULTS AND DISCUSSION

Synthesis. For future X-ray contrast applications, we have developed an aerobic, aqueous solution method for the preparation of chemically and colloidally stable, water-soluble, potentially biologically compatible BiNPs, which should have the following advantages over existing BiNP preparations: (1) it negates the need for phase-transfer steps post-synthesis, (2) it simplifies preparation and purification steps in employing highly biocompatible starting materials, and (3) it reduces overall environmental impact. The starting material, bismuth nitrate pentahydrate, was chosen as an inexpensive, readily available, and easily dissolved (at low pH, or in dilute aqueous solutions) bismuth(III) source. To reduce bismuth(III) to elemental form, sodium borohydride was chosen, because this reducing agent should decompose in aqueous solution to a gaseous product (H_2) and a soluble sodium salt (e.g., $NaBO_2$) that can easily be removed via dialysis. A surface stabilizing ligand or polymer was necessary to achieve chemically and colloidally stable, elemental BiNPs, and in our preparation, the glucose polymer dextran was found to impart both oxidative and colloidal stability to the BiNPs if the particles were formed slowly (i.e., over a duration of 1−10 min). The solubility of the bismuth(III) source as a function of pH was found to dramatically affect the extent of aggregation and colloidal stability of the BiNP products (Scheme 1), which we discuss below.

Scheme 1. pH-Dependent Synthesis of Colloidally Stable Bismuth(0) Glyconanoparticles

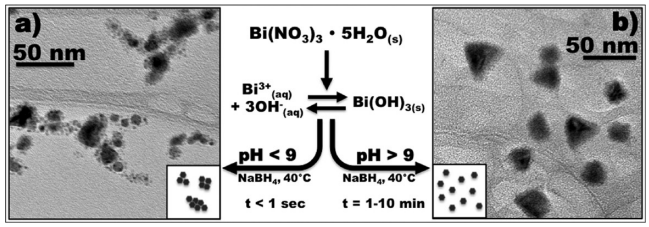

Visibly, we observed a reaction progression in which both nucleation period and growth rate are dependent on synthesis pH. Treatment of a colorless solution or white suspension of $Bi(NO_3)_3 \cdot 5H_2O$ in the presence of glycine and dextran with reducing agent resulted in the evolution of a brown, and, ultimately, a black, solution color (see Figures 1a−e). The

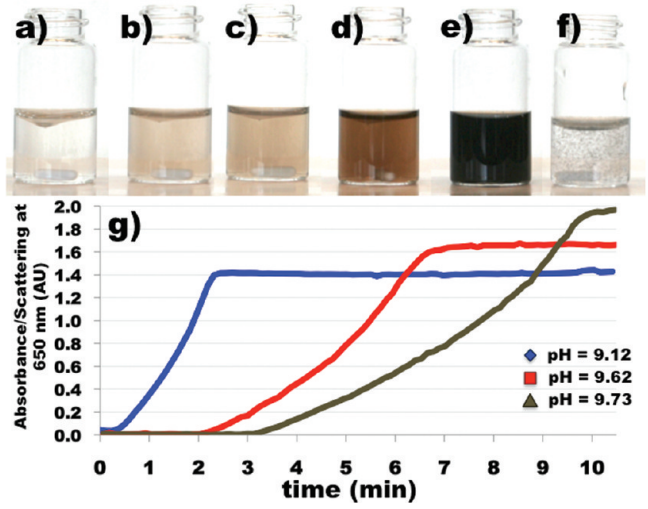

Figure 1. Nucleation period and growth rate are dependent on the reaction pH. (a−f) Treating a colorless solution or white suspension of bismuth nitrate in the presence of glycine and dextran (panel a) with reducing agent leads to the development (panels b−e) of a black colloid of bismuth nanoparticles (panel e) in a time frame that is pH-dependent. Particle synthesis in the absence of surfactant or at pH <8 resulted in unstable aggregates (panel f). (g) Reaction progression monitored by light attenuation at 650 nm for solutions at measured pH values of 9.12 (blue), 9.62 (red), or 9.73 (green).

elapsed time to obtain an initial brown color, indicative of the beginning of particle nucleation, and the elapsed time to obtain the stable black color, indicative of the formation of larger bismuth(0) nanocrystallites, were noticeably longer with increased reaction pH. In the absence of the carbohydrate surfactant, black BiNPs were visibly formed (the rhombohedral bismuth(0) phase was confirmed by powder X-ray diffraction (PXRD)) upon the addition of the reducing agent to the aqueous bismuth(III) precursor; however, these bismuth(0)

dx.doi.org/10.1021/cm300083j | *Chem. Mater.* 2012, 24, 1599−1605

particles quickly aggregated, precipitated out of solution, and eventually underwent oxidation and hydrolysis, resulting in the formation of an unidentified, white amorphous solid. Using glycine as a biocompatible buffering agent with amine pK_a of 9.8 and medical-grade 75 000 MW dextran as a polymeric surface stabilizer, we spectroscopically determined the optimal pH range for the synthesis of colloidally stable, aqueous BiNPs that do not aggregate or decompose to oxidized products (e.g., bismuth(III) solids, such as $Bi(OH)_3$ or Bi_2O_3, or bismuth(III) solution species, such as BiO_2^- or BiO_3^{3-}) for periods as long as 12 months when appropriately (vide infra) stored in aqueous solution.

The effect of pH on the reaction progression and rate is shown in Figure 1g. To monitor the BiNP formation as a function of pH in situ, UV−vis spectroscopy was performed on small-scale preparations using initial reagent concentrations that yielded products with suitable attenuation values (<2 arbitrary units). Light attenuation, the combination of absorption and scattering, at 650 nm was measured and is indicative of the reaction progression, i.e., the formation of black, visible-light-absorbing/scattering particles. The attenuation versus time plots (Figure 1g) indicate that the reactions proceed in three phases: an initial nucleation phase with no attenuation, a particle growth phase indicated by a dramatic increase in attenuation, and finally a steady-state phase indicated by a plateau in attenuation. Under certain conditions, e.g., low pH (<8) syntheses, a fourth aggregation phase is observed (Figure 1f), which is evidenced by loss of attenuation as the particles precipitate (data not shown). The time period of the nucleation phase is strongly pH dependent and is longer at higher pH values. The rate of particle growth, as indicated by the change in attenuation with time (i.e., the slope of the growth regime in Figure 1g), is also pH-dependent and is slower at higher pH values. Regardless of synthesis pH, all samples reach an absorbance plateau corresponding to a steady-state phase in which the composition of the solution does not appear to change with time. Experimentally, we observed that, at a low reaction pH (≤8.0), large aggregates of elemental Bi particles were formed in the presence of dextran; these aggregated particles did not oxidize or decompose, as evidenced by the black color of the precipitated solid and confirmation of the rhombohedral bismuth(0) phase by PXRD. However, the large aggregates of elemental BiNPs synthesized at pH ≤ 8.0 could not be redispersed in water, even with durative sonication, to achieve stable aqueous colloids. We found that increasing the reaction pH (up to pH 10.5) produced a greater number of isolated BiNPs (see Scheme 1) that did not undergo gravitational settling, thus resulting in stable, aqueous Bi glyconanoparticle colloids. At pH >11, no reaction was observed visually or spectroscopically, presumably because of the lack of soluble bismuth(III) for reduction (vide infra). For colloidally stable samples synthesized in solutions with pHs between 9 and 10, dilute phosphoric acid was added dropwise to achieve final solutions at a physiologically relevant pH of 7.4 without a loss of either colloidal or chemical stability.

A nanoparticle formation mechanism consistent with the pH effects that we observe in the aqueous synthesis is shown in Scheme 1. For simplicity, we assume that a suspension of solid bismuth hydroxide is in equilibrium with aqueous bismuth(III) and hydroxide ions and that the equilibrium is dependent on pH, with a decreased bismuth(III) concentration achieved by increasing pH according to LeChatlier's principle. When the soluble bismuth(III) precursor is depleted by reaction with the reducing agent to form bismuth(0) nanoparticles, the solid equilibrium shifts to replenish the solution precursor at the expense of the precipitate. Thus, the pH-dependent dissolution of the solid should allow for kinetic control over BiNP nucleation and growth by modulating the concentration of soluble bismuth(III) monomer available for reduction. Consistent with this, we observe that both nucleation and growth are faster the lower the synthesis pH, which is correspondent with higher available bismuth(III) concentration for reduction in more acidic solutions. Also consistent with this, at pH ≤8, not enough isolated bismuth(0) nanoparticles are formed to result in a stable aqueous colloid, because the saturation concentration for nucleation and growth is achieved too rapidly, resulting in the formation and precipitation of aggregated nanocrystallites. Notably, the largest difference in the reaction products synthesized at different pH values is not the individual bismuth nanocrystallite size, but the extent of nanocrystallite aggregation, and thus the size and weight of the Bi glyconanoparticles (where a Bi glyconanoparticle can contain one or more than one Bi nanocrystallite). If Bi nanocrystals are formed quickly, as occurs in the lowest pH reactions, this presents opportunities for multiple nanocrystalline domains to be encapsulated within a single polymeric structure. However, if particles are formed slowly, there are fewer present in solution at any given time prior to particle capping (a fast step) by the polymer, thus reducing the opportunity for inclusion of multiple Bi nanocrystals in a single polymer structure and, consequently, reducing the Bi glyconanoparticle size and tendency for gravitational settling.

Thus, the pH dependence of BiNP colloidal stability is influenced by a complex pH-dependent solubility equilibrium involving sparingly soluble bismuth(III) oxide, suboxide, hydroxide, or perhaps, in this case, glycinate precipitates. Depending on the counteranion, a wide range of oxidized precipitates have been reported for dissolved bismuth(III) salts.[32] Although we made no attempts to identify either the precipitate or the solution precursor, bismuth(III) is known to form a highly acidic (pK_a = 1.1) aquo-cation in dilute solution; in concentrated solution or upon titration with base, aqueous bismuth(III) is expected to form an insoluble basic salt that will be in pH-dependent equilibrium with a soluble bismuth(III) species.[31,33] Consistent with this, the Pourbaix diagram for bismuth in aerated water indicates that the predominant form of bismuth will be an oxidized solid over most of the pH range.[34] A titration curve for $Bi(NO_3)_3{\cdot}5H_2O$ (see Figure S1 in the Supporting Information) indicates that the onset of precipitation in dilute solution (2.42 mM) occurs at pH ∼4 and prior to the addition of 3 mol equiv of hydroxide. Qualitatively, the same results were observed when $Bi(NO_3)_3{\cdot}5H_2O$ was titrated in the presence of glycine; thus, we expected and observed a significant amount of solid precipitated precursor in our syntheses at all tested pHs. Further details of aqueous bismuth chemistry can be found in the Supporting Information. However, regardless of the identity of the solution precursor and sparingly soluble solid, controlling the pH will control the bismuth(III) concentration available for reduction, which is consistent with our spectroscopic observations and proposed, aqueous formation mechanism. Notably, the successful aqueous synthesis of hydrophobic, oleate-capped BiNPs was performed under basic conditions using hydrazine hydrate.[30]

The impact of a variety of other synthetic factors on particle formation kinetics and product colloidal stability was measured

spectroscopically, including the addition of salts (e.g., NaCl, KNO_3), buffering agents other than glycine (e.g., bicine, tris), and buffer concentration. In all cases, we observed a pH-dependent nucleation and growth period with the colloidal stability correlated to synthesis pH more than any other factor and with the most stable colloids achieved in solutions between pH values of 9 and 10. We anticipate exploring other kinetic details of this reaction in the future, specifically focusing on reducing the hydrodynamic radius to Bi nanocrystallite size (see the Characterization section) by changing surfactant concentration and/or molecular weight.

Characterization. Transmission electron microscopy (TEM) was used to analyze BiNP morphology, size, and crystallinity (see Figures 2a and 2b). Various crystallite morphologies were observed, regardless of synthesis pH, including spheres, triangles, hexagons, and rods. However, >50% of particles were spherical in all cases. TEM images of colloids synthesized at a pH of 9.97 indicate a mean free-standing particle diameter of 19.5 ± 3.7 nm (Figure 2c). Under high-resolution TEM, a lattice spacing of 0.332 nm was measured (see Figure 2d), which is consistent with the *d*-spacing (0.328 nm) corresponding to the [012] planes of bulk elemental bismuth (JCPDS Card No. 00-044-1246). EDX analysis was performed on 20 isolated particles using the same sample grid and only the elements Bi, O, C, and Cu (from the grid support) were found. The presence of bismuth was localized to the particles, i.e., no bismuth was detected outside of the dark crystallites visible on the TEM grid.

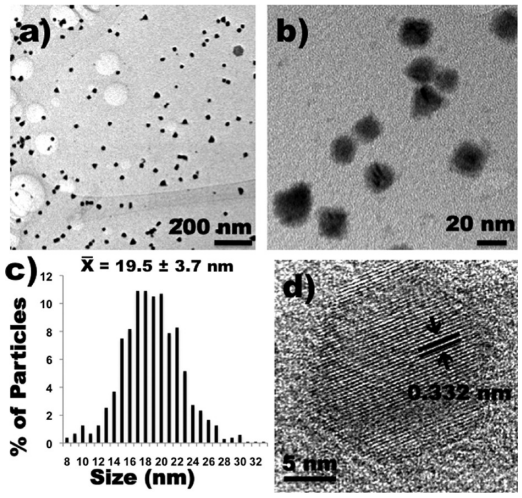

Figure 2. (a, b, d) Transmission electron microscopy (TEM) images of bismuth nanoparticles synthesized at pH 9.97: (a,b) the majority of particles appear spherical, although triangles, cubes, and hexagons are also visible; (d) high-resolution TEM image of a single particle with line spacing (3.32 Å) characteristic of elemental bismuth. Panel (c) is a histogram showing that 1040 particles were manually measured; the mean diameter is 19.5 ± 3.7 nm.

The dried colloids were analyzed by PXRD, and the resulting diffraction pattern is that of rhombohedral elemental bismuth (see blue trace in Figure 3a, JCDPS Card No. 00-044-1246; tick marks indicate calculated reflections), which is consistent with the high-resolution TEM analysis. Other reflections apparent in the pattern (17.52°, 18.83°, 20.25°, and 28.80° 2Θ) were attributed to crystallized dextran (purple trace in Figure 3a).

The FT-IR spectrum (Figure 3b) of the dialyzed particles (blue) matched the spectrum collected for neat dextran

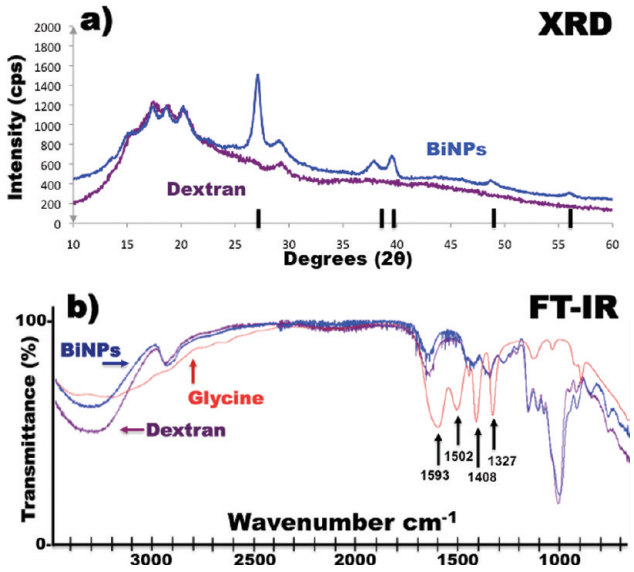

Figure 3. (a) Powder X-ray diffraction (PXRD) shows BiNPs (blue trace) to be composed of crystallized dextran (purple trace) and elemental bismuth (calculated Bragg reflections for rhombohedral Bi indicated by tick marks). (b) FT-IR spectra of purified, dextran-stabilized BiNP thin films (blue trace), glycine (red trace), and dextran (purple trace).

(purple). Importantly, the absence of carboxylate peaks at 1593 and 1408 cm^{-1} and amine deformation peaks at 1527 and 1502 cm^{-1} [35] suggests that glycine served only as a buffering reagent during synthesis and did not become part of the BiNP complex. This was somewhat surprising, given that oleic acid and other carboxylate-containing species are commonly observed to be surface-terminating ligands in other BiNP preparations.[30,36] Particles appear to be coated solely in dextran and thus can be accurately termed bismuth glyconanoparticles.

Dynamic light scattering (DLS) measurements on colloids synthesized at pH 9.97 indicated the mean hydroynamic diameter to be 130 nm when filtered through a 0.45-μm syringe filter. The difference (~110 nm) between the crystallite size (diameter = 19.5 nm) measured by TEM and hydrodynamic radius (130 nm) measured by DLS can be attributed to a surfactant and water shell, which presumably imparts colloidal stability and solubility to the particles and prevents or slows hydrolysis and oxidation. DLS data, in comparison with TEM data, are shown in Figure S2 in the Supporting Information.

Stability and Degradation. To examine the colloidal stability of the BiNPs over time, purified and concentrated BiNPs were redispersed in aqueous solutions of varying pH using 1.0 M phosphoric acid adjusted with KOH to achieve specified pH values in the range of 2−12; these samples were protected from light. In addition, two samples were redispersed in water; one was stored in darkness and the other was exposed to sunlight. Visual observation (Figures 4a−c) and UV−vis spectroscopy (Figure 4d) were used to monitor the stability of the colloids, which was indicated by the maintenance of a dark solution color and the absence of precipitates.

When BiNPs were introduced to the pH 2 solution, the particles immediately dissolved, as evidenced by the loss of solution color and the absence of precipitate. Samples in solutions with pH values of 4, 6, 7, and 12 initially retained their color, but fully dissolved to yield colorless solutions within 24 h; the low pH results suggest that the acidic environment of a

dx.doi.org/10.1021/cm300083j | *Chem. Mater.* 2012, 24, 1599−1605

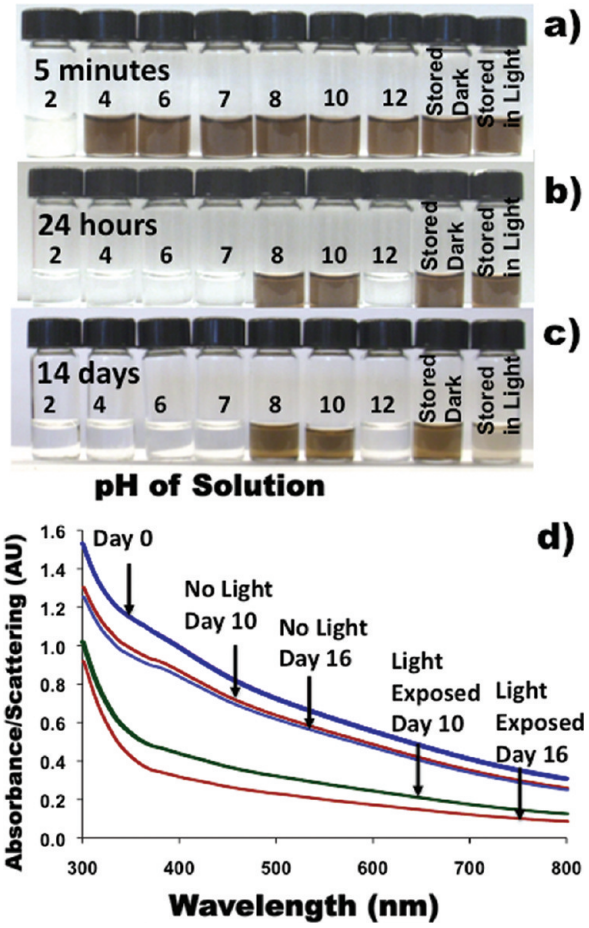

Figure 4. (a–c) For pH stability experiments, purified bismuth nanoparticles (BiNPs) (dialyzed, centrifuged, and concentrated) were diluted in 1.0 M phosphate solutions and the pH was adjusted with KOH to achieve solutions ranging in pH from 2 to 12; light/dark controls were diluted in water and visually analyzed at the same time points. All vials were examined for solution color and presence/absence of precipitates at time points of (a) 5 min, (b) 24 h, and (c) 14 days. (d) For spectroscopically monitored light stability experiments, purified colloids were diluted in H_2O and spectra taken at time points of 0, 10, and 14 days. Light-exposed samples were placed in vials in direct sunlight and all other samples were stored in vials wrapped in aluminum foil; absorbance was monitored at 650 nm.

lysosome would decompose these particles in vivo. However, samples redispersed in solutions at pH 8 and pH 10 were colloidally stable for over one month, as was a control sample that was diluted in nanopure water. The latter result suggests that phosphate ions may assist degradation over some pH range, but the effect of ion identity and solution ionic strength was not further examined.

Photodegredation was examined by preparing two samples of dilute colloidal solutions of BiNPs in glass scintillation vials. One sample was exposed to ambient light, and one sample was protected from light by a single layer of aluminum foil. Both samples were placed side by side in a window, and after 2 weeks, the sample that was exposed to light had decreased in color intensity (Figure 4c). To spectroscopically monitor for photodegradation, a dilute solution of BiNPs was initially divided into two cuvettes and the UV–visible spectrum of each was recorded daily over a period of 16 days (Figure 4d). One cuvette was wrapped in aluminum foil and both cuvettes were placed in direct sunlight; care was taken not to agitate the samples between measurements, in case some settling of particles or precipitate formation occurred. Initially, both samples showed identical broad absorption spectra, covering the entire visible range with shoulders in the absorption spectra apparent ~375 nm. The sample constantly exposed to light lost absorbance intensity uniformly across the visible spectrum, and changed from a dark solution to a light brown solution slowly over the course of several days. Conversely, the sample that was stored in darkness appeared to be much more stable, as evidenced by a much slower loss of color over time. The photoinstability of these particles is unsurprising given their high visible light absorption cross-section and may indicate an alternative clearance route for elemental BiNPs employed as XCAs.

The BiNP colloids were also tested for temperature stability by freezing and boiling BiNP samples redispersed in nanopure water. BiNP samples diluted in water and heated to boiling for greater than an hour remained colloidally stable, without loss of solution color or formation of precipitates. In addition, water-dispersed BiNPs were slowly frozen at −20 °C and rapidly frozen in liquid nitrogen; neither treatment reduced the color or colloidal stability of the particle solutions upon thawing, indicating that the Bi glyconanoparticle colloids are robust over a wide range of temperatures.

■ CONCLUSION

The recent popularity of green chemical techniques has put an emphasis on using water as a solvent for the synthesis of nanomaterials, and water solubility and stability is required for nanomaterial X-ray contrast agents (XCAs). These features are difficult to achieve in oxidatively prone elements such as bismuth. Furthermore, the synthesis of elemental nanomaterials by reduction of cations often requires a strong reducing agent and controlled kinetics to avoid formation of bulk materials and to promote uniform particle growth. Herein, we have described a synthesis method that takes advantage of a sparingly soluble solid to kinetically slow the formation and growth of bismuth nanoparticles (BiNPs) in water by controlling the pH, and thus the concentration of bismuth(III) monomer in solution available for reduction. The method allows sufficiently slow growth at modestly basic pH values (pH 8–10) to result in isolated and colloidally stable, rather than aggregated and precipitated, BiNPs. The glucose polymer dextran is used to surface stabilize the nanoparticles and promote chemical and colloidal stability. The Bi(0) glyconanoparticles can be purified and redispersed in water or in a mildly basic phosphate buffer, and these solutions are then stable for months when stored away from light.

In summary, chemically and colloidally stable, elemental bismuth glyconanoparticles have been synthesized using a simple, pH-controlled, aqueous method. These high-atomic-number Bi(0) glyconanoparticles have size, solubility, and stability characteristics suitable for use as nanomaterial XCAs. Bismuth is known to be both highly X-ray attenuating and biologically compatibility, which makes elemental BiNPs good candidates for in vivo nanoscale XCAs. We anticipate future experimentation with these particles to include toxicity evaluation and determination of X-ray attenuation coefficients at diagnostic X-ray voltages.

dx.doi.org/10.1021/cm300083j | *Chem. Mater.* 2012, 24, 1599–1605

■ ASSOCIATED CONTENT

Supporting Information

Titration data for bismuth nitrate pentahydrate and dynamic light scattering (DLS) versus transmission electron microscopy (TEM) comparison of syringe filtered Bi(0) glyconanoparticles. This material is available free of charge via the Internet (as PDF) at http://pubs.acs.org.

■ AUTHOR INFORMATION

Corresponding Author

*E-mail: agoforth@pdx.edu.

Notes

The authors declare no competing financial interest.

■ ACKNOWLEDGMENTS

We would like to acknowledge the Portland State University Center for Electron Microscopy and Nanofabrication (CEMN) for microscopy access and technical support. We also thank Dr. W. Alexander Merrill and Dr. F. Andrew Frame for their comments and suggestions. Financial support for this project was provided by the Burroughs Wellcome Fund (Award No. 1007294.01; author A.M.G. holds a Career Award at the Scientific Interface from the Burroughs Wellcome Fund), the Oregon Nanoscience and Microtechnologies Institute (Task Order No 3. of the Master Grant Agreement, author A.M.G. is a Signature Research Fellow), and Portland State University. Finally, we thank the National Science Foundation for PXRD instrumentation (NSF-MRI, Award No. DMR-0923572).

■ REFERENCES

(1) Zhang, Z.; Ying, J. Y.; Dresselhaus, M. S. *J. Mater. Res.* **1998**, *13*, 1745−1748.
(2) Wang, Y. W.; Kim, J. S.; Kim, G. H.; Kim, K. S. *Appl. Phys. Lett.* **2006**, *88*, 143106.
(3) Heremans, J.; Thrush, C. M. *Phys. Rev. B* **1999**, *59*, 12579.
(4) Boukai, A.; Xu, K.; Heath, J. R. *Adv. Mater.* **2006**, *18*, 864−869.
(5) Fanfair, D. D.; Korgel, B. A. *Cryst. Growth Des.* **2005**, *5*, 1971−1976.
(6) Wang, F.; Tang, R.; Kao, J. L.-F.; Dingman, S. D.; Buhro, W. E. *J. Am. Chem. Soc.* **2009**, *131*, 4983−4994.
(7) Chockla, A. M.; Harris, J. T.; Korgel, B. A. *Chem. Mater.* **2011**, *23*, 1964−1970.
(8) Rabin, O.; Manuel Perez, J.; Grimm, J.; Wojtkiewicz, G.; Weissleder, R. *Nat. Mater.* **2006**, *5*, 118−122.
(9) Pan, D.; Roessl, E.; Schlomka, J.; Caruthers, S. D.; Senpan, A.; Scott, M. J.; Allen, J. S.; Zhang, H.; Hu, G.; Gaffney, P. J.; Choi, E. T.; Rasche, V.; Wickline, S. A.; Proksa, R.; Lanza, G. M. *Angew. Chem.* **2010**, *122*, 9829−9833.
(10) Ai, K.; Liu, Y.; Liu, J.; Yuan, Q.; He, Y.; Lu, L. *Adv. Mater.* **2011**, *23*, 4886−4891.
(11) Choi, H. S.; Liu, W.; Misra, P.; Tanaka, E.; Zimmer, J. P.; Ipe, B. I.; Bawendi, M. G.; Frangioni, J. V. *Nat. Biotechnol.* **2007**, *25*, 1165−1170.
(12) Mammen, M.; Choi, S.; Whitesides, G. M. *Angew. Chem., Int. Ed.* **1998**, *37*, 2754−2794.
(13) Briand, G. G.; Burford, N. *Chem. Rev.* **1999**, *99*, 2601−2658.
(14) Hainfeld, J. F.; Slatkin, D. N.; Focella, T. M.; Smilowitz, H. M. *Br. J. Radiol.* **2006**, *79*, 248−253.
(15) Popovtzer, R.; Agrawal, A.; Kotov, N. A.; Popovtzer, A.; Balter, J.; Carey, T. E.; Kopelman, R. *Nano Lett.* **2008**, *8*, 4593−4596.
(16) Eck, W.; Nicholson, A. I.; Zentgraf, H.; Semmler, W.; Bartling, S. *Nano Lett.* **2010**, *10*, 2318−2322.
(17) *Free Bismuth Price Charts*. http://www.metalprices.com/pubcharts/Public/Bismuth_Price_Charts.asp (accessed Aug. 8, 2011).
(18) Greenwood, N. N.; Earnshaw, A. In *Chemistry of the Elements*, 2nd Ed.; Butterworth−Heinemann: Oxford, U.K., 1998; pp 547−600.
(19) Cormode, D. P.; Skajaa, T.; Fayad, Z. A.; Mulder, W. J. M. *Arterioscler. Thromb. Vas.* **2009**, *29*, 992−1000.
(20) Longmire, M.; Choyke, P. L.; Kobayashi, H. *Nanomedicine−U.K.* **2008**, *3*, 703−717.
(21) Bierer, D. W. *Rev. Infect. Dis.* **1990**, *12* (Suppl. 1), S3−S8.
(22) Sun, H.; Li, H.; Harvey, I.; Sadler, P. J. *J. Biol. Chem.* **1999**, *274*, 29094−29101.
(23) Yu, H.; Gibbons, P. C.; Buhro, W. E. *J. Mater. Chem.* **2004**, *14*, 595.
(24) Wang, F.; Tang, R.; Yu, H.; Gibbons, P. C.; Buhro, W. E. *Chem. Mater.* **2008**, *20*, 3656−3662.
(25) Richards, V. N.; Shields, S. P.; Buhro, W. E. *Chem. Mater.* **2011**, *23*, 137−144.
(26) Wang, Y.; Xia, Y. *Nano Lett.* **2004**, *4*, 2047−2050.
(27) Li, J.; Fan, H.; Chen, J.; Liu, L. *Colloid Surf. A* **2009**, *340*, 66−69.
(28) Wang, F.; Tang, R.; Yu, H.; Gibbons, P. C.; Buhro, W. E. *Chem. Mater.* **2008**, *20*, 3656−3662.
(29) Wang, Y.; Kim, K. S. *Nanotechnology* **2008**, *19*, 265303.
(30) Wang, Y.; Zhao, J.; Zhao, X.; Tang, L.; Li, Y.; Wang, Z. *Mater. Res. Bull.* **2009**, *44*, 220−223.
(31) Irmawati, R.; Noorfarizan Nasriah, M. N.; Taufiq-Yap, Y. H.; Abdul Hamid, S. B. *Catal. Today* **2004**, *93*−*95*, 701−709.
(32) Kragten, J.; Decnop-Weever, L. G.; Gründler, P. *Talanta* **1993**, *40*, 485−490.
(33) Schumb, W. C.; Rittner, E. S. *J. Am. Chem. Soc.* **1943**, *65*, 1055−1060.
(34) Wulfsberg, G. In *Inorganic Chemistry*; University Science Books: Sausalito, CA, 2000; p 293.
(35) Suzuki, S.; Shimanouchi, T.; Tsuboi, M. *Spectrochim. Acta* **1963**, *19*, 1195−1208.
(36) Yarema, M.; Kovalenko, M. V.; Hesser, G.; Talapin, D. V.; Heiss, W. *J. Am. Chem. Soc.* **2010**, *132*, 15158−15159.